

DIAGRAMMI DI FASE

α β Coesistenza: $T_\alpha = T_\beta$, $P_\alpha = P_\beta$, $\mu_\alpha = \mu_\beta$

Potenziale di Gibbs: $G = E - TS + PV$

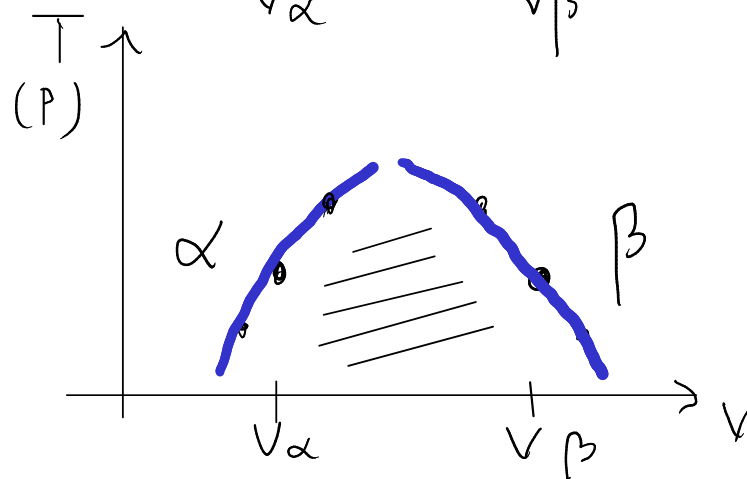
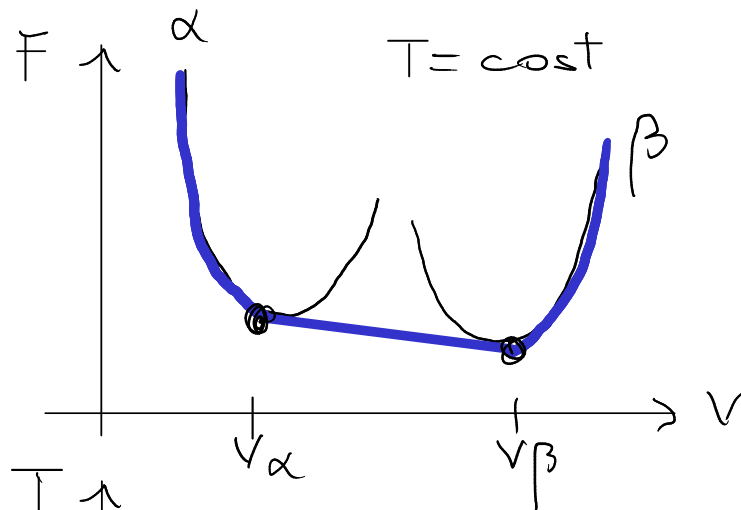
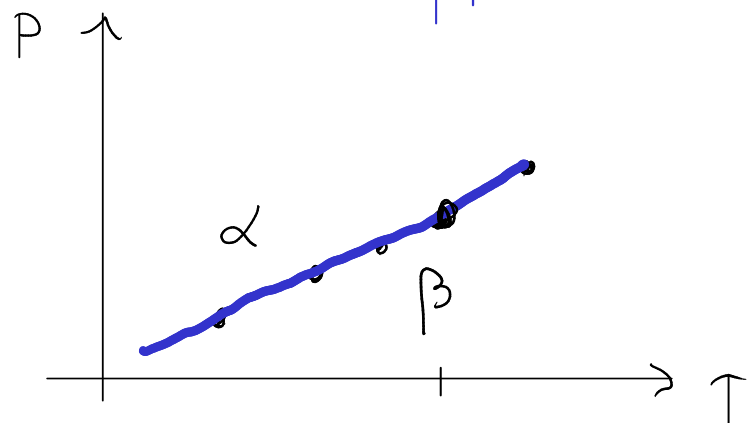
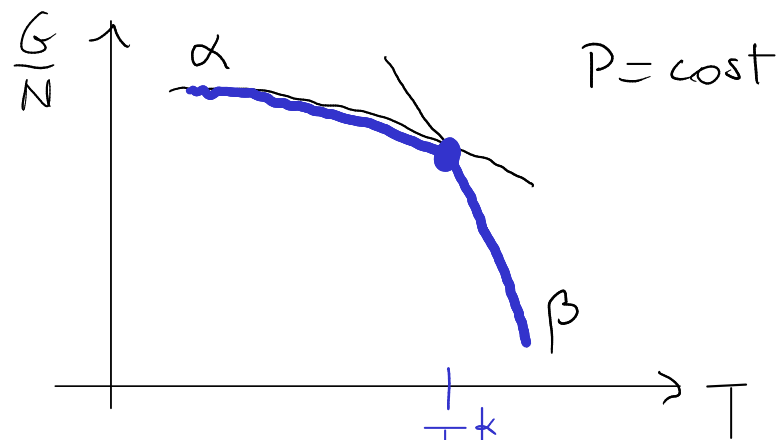
P, T fissate. Equilibrio: minimo G

$\mu = \frac{G}{N}$ $g_\alpha = \frac{G_\alpha}{N}$ $dG = VdP - SdT$

Potenziale di Helmolte: $F = E - TS$

V, T fissati, Equilibrio: minimo F

$dF = -PdV - SdT$



Eq. Clausius - Clapeyron

$$\frac{dP}{dT} \approx \frac{L_{\alpha \rightarrow \beta}}{(v_{\beta} - v_{\alpha})T} \rightarrow \text{calore latente } \alpha \rightarrow \beta$$

↑ ↑
volume specific
 $v = V/N$

Common tangent construction

$$\left(\frac{dF}{dV} \Big|_{V_{\alpha}} = \frac{dF}{dV} \Big|_{V_{\beta}} \quad (P_{\alpha} = P_{\beta}) \right.$$

$$\left. F(V_{\alpha}) = F(V_{\beta}) + \frac{dF}{dV} \Big|_{V_{\beta}} (V_{\alpha} - V_{\beta}) \right.$$

$$F(V_{\alpha}) - \frac{dF}{dV} \Big|_{V_{\alpha}} V_{\alpha} = F(V_{\beta}) - \frac{dF}{dV} \Big|_{V_{\beta}} V_{\beta}$$

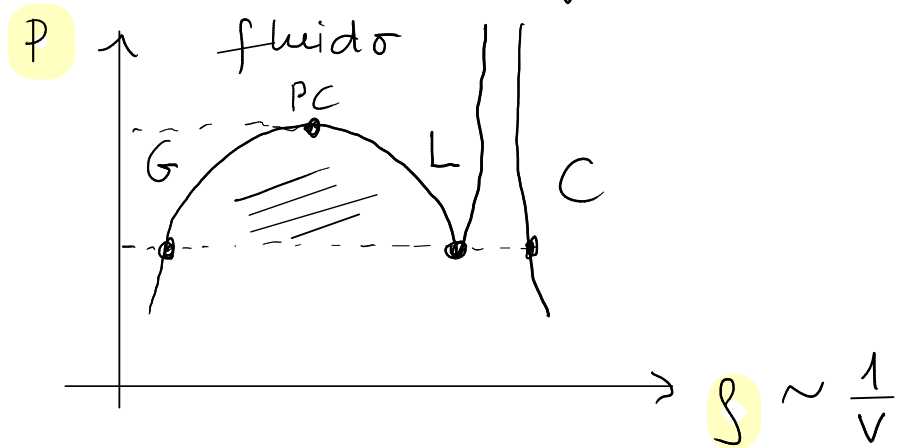
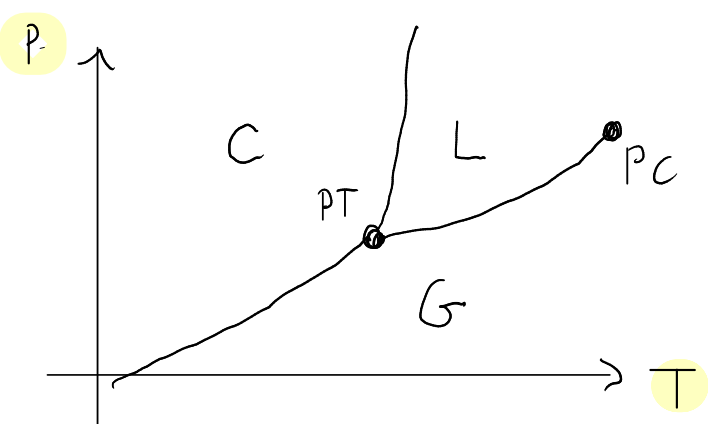
$$F_{\alpha} + P_{\alpha} V_{\alpha} = F_{\beta} + P_{\beta} V_{\beta}$$

$$G_{\alpha} = G_{\beta}$$

TOPOLOGIA DEI DIAGRAMMI DI FASE

Sistemi atomici / molecolari mono-componente

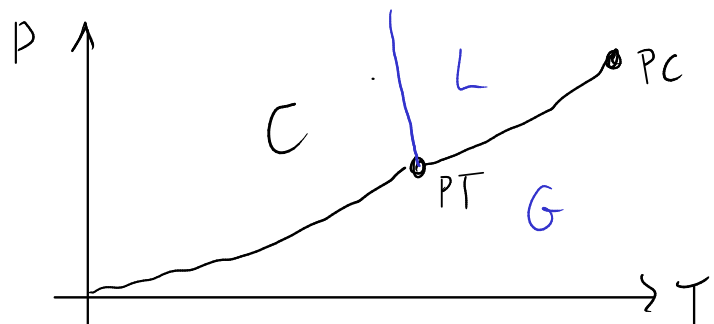
1. Sistemi "normali" : es.: Argon



$$\frac{dP}{dT} = \frac{L_{\alpha\beta}}{T(\nu_{\beta} - \nu_{\alpha})} \quad \begin{matrix} \alpha = C \\ \beta = L \end{matrix}$$

$$\left. \begin{matrix} L_{CL} > 0 \\ T > 0, \nu_L - \nu_C > 0 \end{matrix} \right\} \Rightarrow \frac{dP}{dT} > 0$$

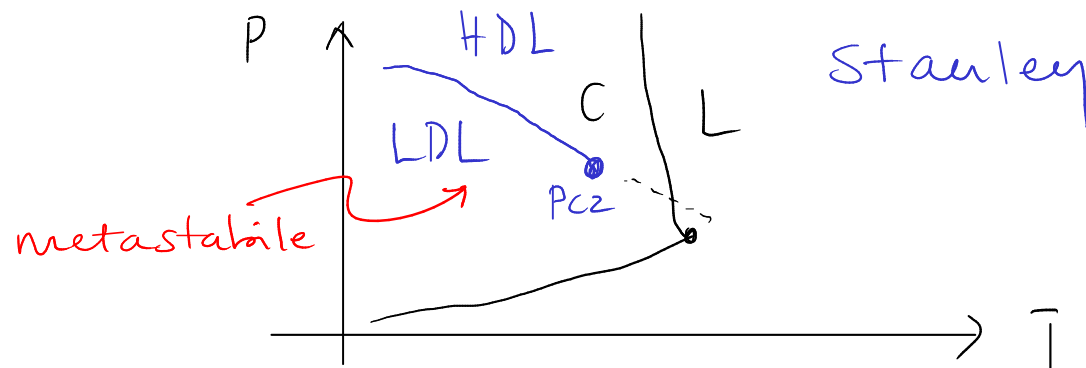
2. Sistemi "anomali" : es.: H₂O, Si, Ge



$$\frac{dP}{dT} < 0$$

$$L_{CL} > 0, \nu_L - \nu_C < 0$$

3. Transizioni liquido-liquido
es. H₂O, Si, Ge, P, S, ...



Princeton

214505-6 Liu *et al.*

J. Chem. Phys. **137**, 214505 (2012)

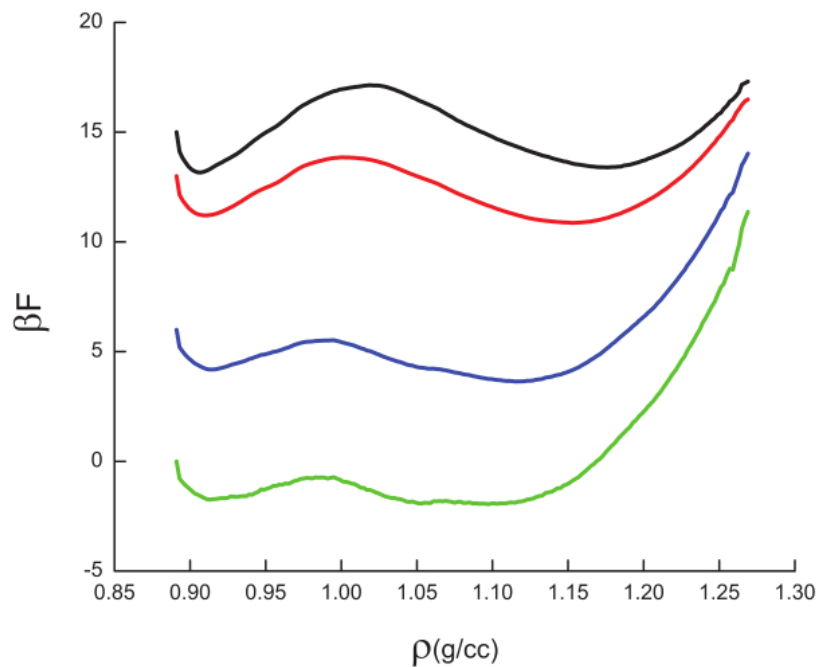


FIG. 4. Density dependence of the contracted free energy obtained by integrating over Q_6 [see Eq. (7)] at phase coexistence conditions. Black curve: 224 K, 2.3 kbar; red curve: 228.6 K, 2.19 kbar; blue curve: 235 K, 2.0 kbar; green curve: 238 K, 1.9 kbar. The relative vertical location of each isotherm is arbitrary.

consistent with free energy vs. density calculations on the ST2 model using reaction field treatment of long-ranged electrostatic interactions.⁶²

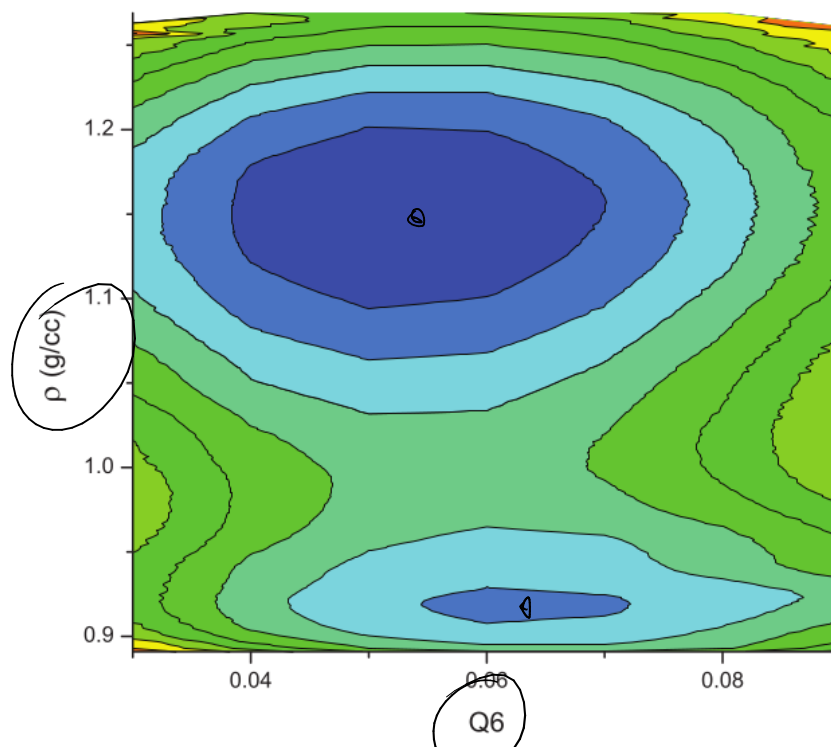
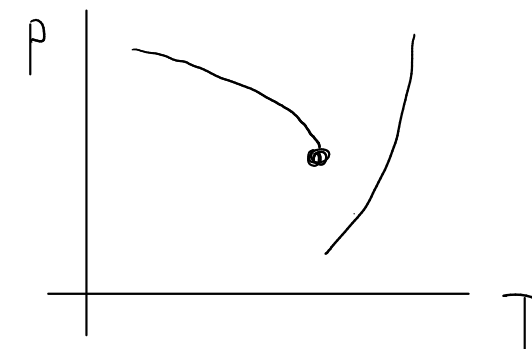
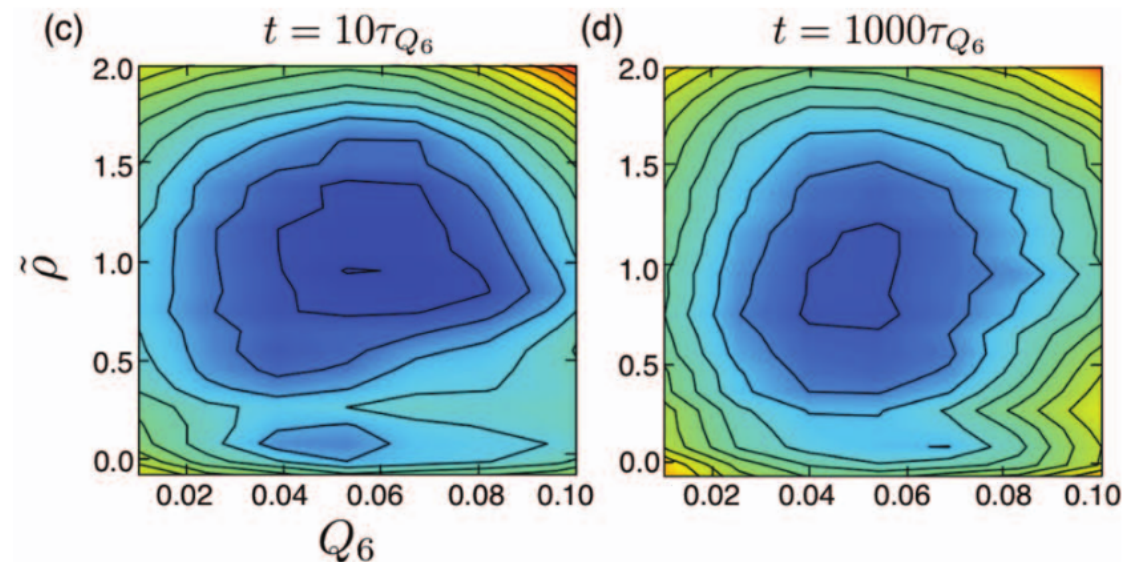


FIG. 6. Free energy surface in the (ρ, Q_6) plane at (228.6 K, 2.2 kbar), calculated with the same HDL-region histograms used to generate Figure 2 and separate LDL-region histograms obtained from simulations in the LDL windows ($0.90 \leq \rho^* \leq 0.94$ g/cc) that were first started from HDL configurations ($1.13 \leq \rho^* \leq 1.16$ g/cc) and subsequently biased to the LDL region. The agreement with the free energy surface shown in Figure 2 is an indication that the simulations properly sample equilibrated phases.

Berkeley

214504-3 D. T. Limmer and D. Chandler J. Chem. Phys. **138**, 214504 (2013)



Sphere dure.

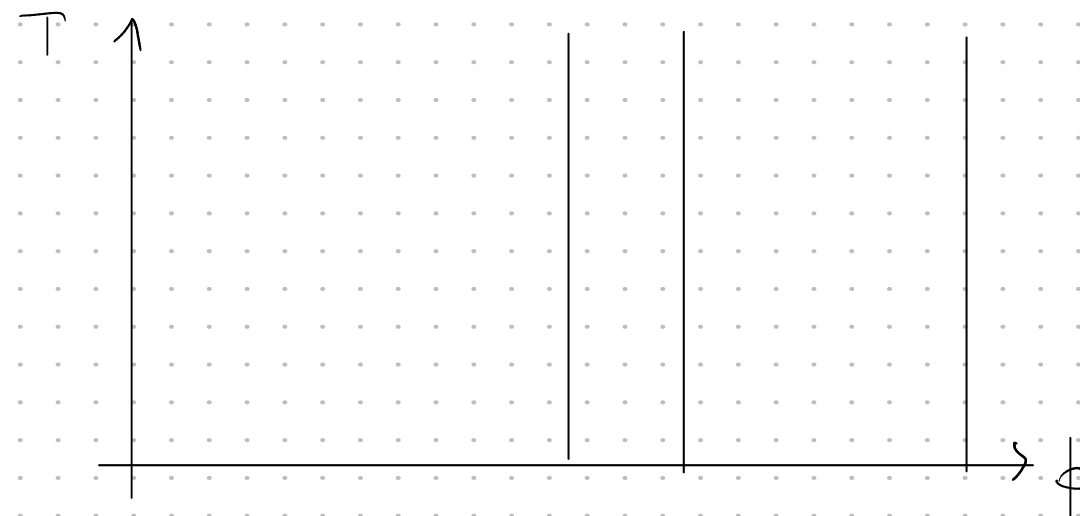
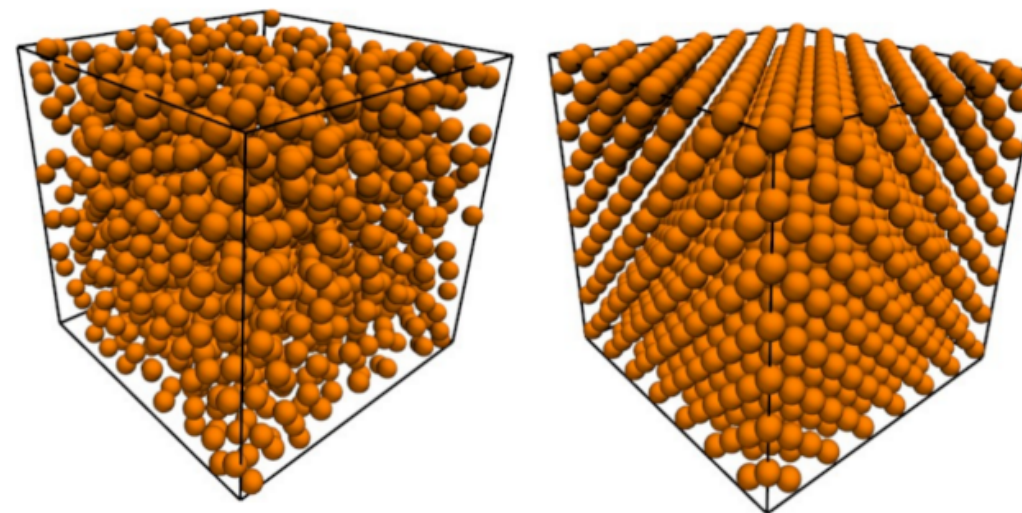
Phase Transition for a Hard Sphere System

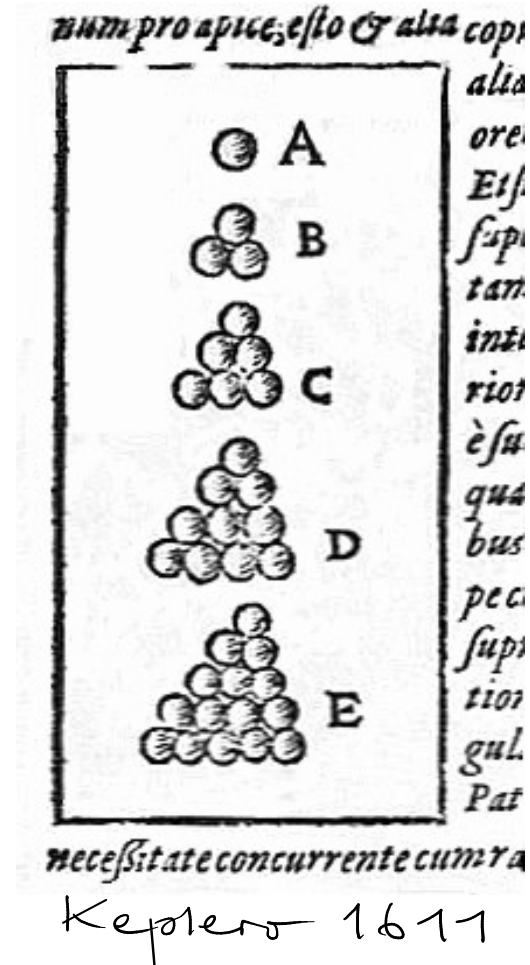
B. J. ALDER AND T. E. WAINWRIGHT

University of California Radiation Laboratory, Livermore, California

(Received August 12, 1957)

A CALCULATION of molecular dynamic motion has been designed principally to study the relaxations accompanying various nonequilibrium phenomena. The method consists of solving exactly (to the number of significant figures carried) the simultaneous classical equations of motion of several hundred particles by means of fast electronic computers. Some of the





Conggettura di
Keplero

Fcc
(HCP)

74%

When presenting the progress of his project in 1996, Hales said that the end was in sight, but it might take "a year or two" to complete. In August 1998 Hales announced that the proof was complete. At that stage, it consisted of 250 pages of notes and 3 gigabytes of computer programs, data and results.

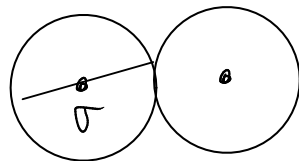
Despite the unusual nature of the proof, the editors of the *Annals of Mathematics* agreed to publish it, provided it was accepted by a panel of twelve referees. In 2003, after four years of work, the head of the referee's panel, Gábor Fejes Tóth, reported that the panel were "99% certain" of the correctness of the proof, but they could not certify the correctness of all of the computer calculations.

Hales (2005) published a 100-page paper describing the non-computer part of his proof in detail. Hales & Ferguson (2006) and several subsequent papers described the computational portions. Hales and Ferguson received the Fulkerson Prize for outstanding papers in the area of discrete mathematics for 2009.

Sfere dure

3d, mono-disperse, $u^{(1)}(\vec{r}) = 0$

$$u_{HS}(r) = \begin{cases} \infty & r \leq \sigma \\ 0 & r > \sigma \end{cases}$$



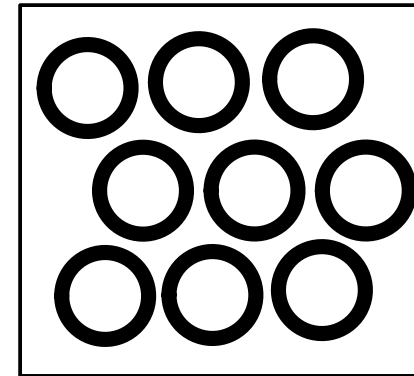
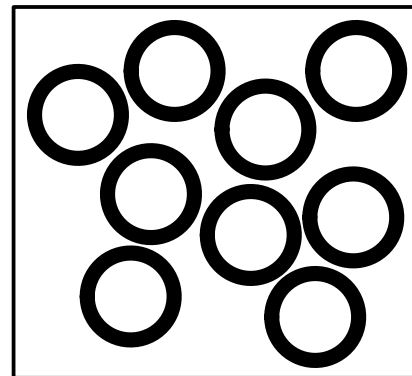
$$\exp \left[-\beta \sum_{i,j} u_{HS}(r_{ij}) \right] = \begin{cases} 1 & \text{no overlap} \\ 0 & \text{overlap} \end{cases}$$

atermico

Frazione di impaccamento

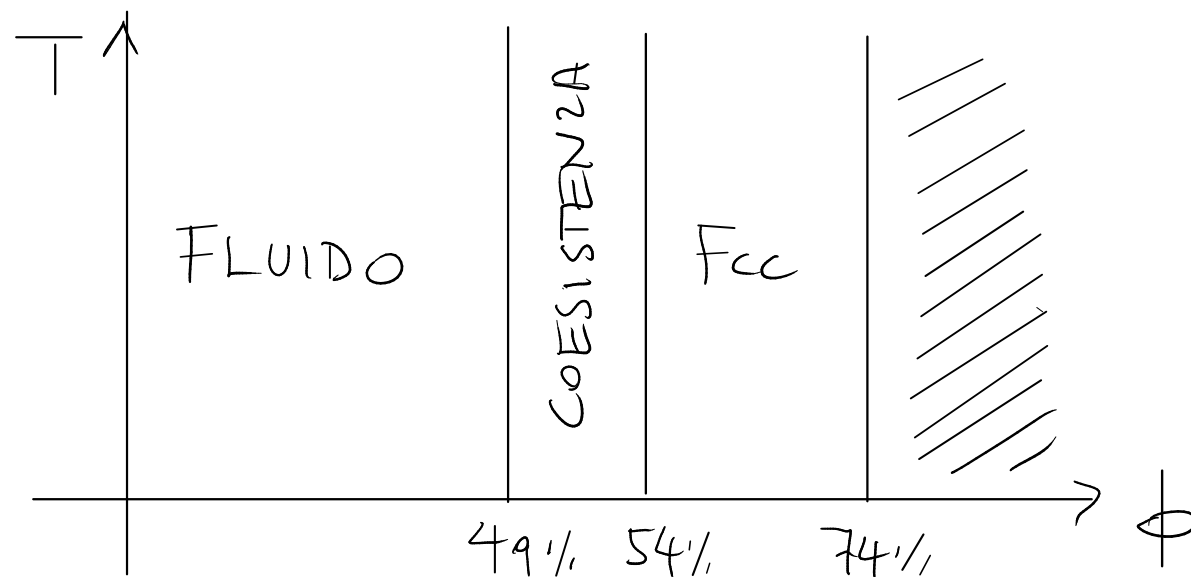
$$\phi \equiv \frac{N \frac{4}{3} \pi (\sigma/2)^3}{V} = \frac{\pi}{6} \sigma^3 \rho$$

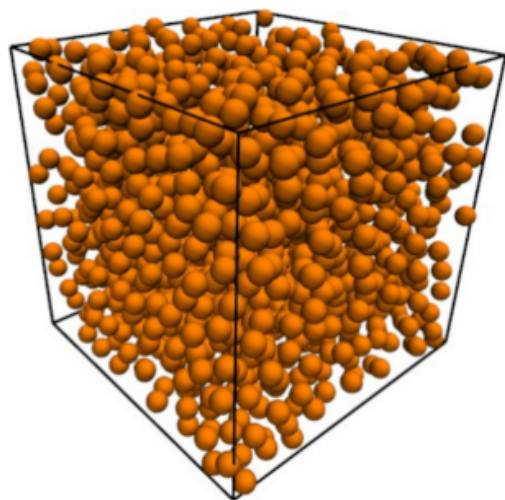
V, T



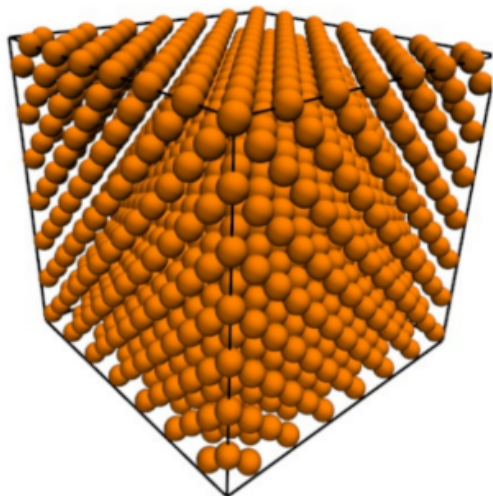
$$F = \cancel{E} - TS$$

$$\phi > \phi_* : S_{FCC} > S_{FLUIDO}$$





FLUIDO



Fcc

Phase Transition for a Hard Sphere System

B. J. ALDER AND T. E. WAINWRIGHT

University of California Radiation Laboratory, Livermore, California

(Received August 12, 1957)

A CALCULATION of molecular dynamic motion has been designed principally to study the relaxations accompanying various nonequilibrium phenomena. The method consists of solving exactly (to the number of significant figures carried) the simultaneous classical equations of motion of several hundred particles by means of fast electronic computers. Some of the



Alder

Diagrammi di fase dei materiali soffici

1. Colloidi duri

Pusey Van Meegen Science 1986

PMMA

$$R = 305 \pm 10 \text{ nm} \quad (3\%)$$

stabilizzazione sterica

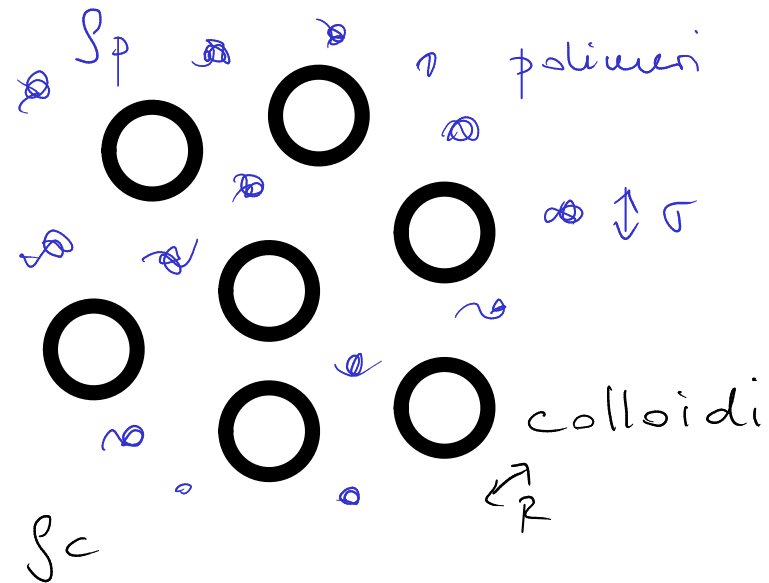
index matching \Rightarrow no vdw



HS



2. Colloidi attrattivi

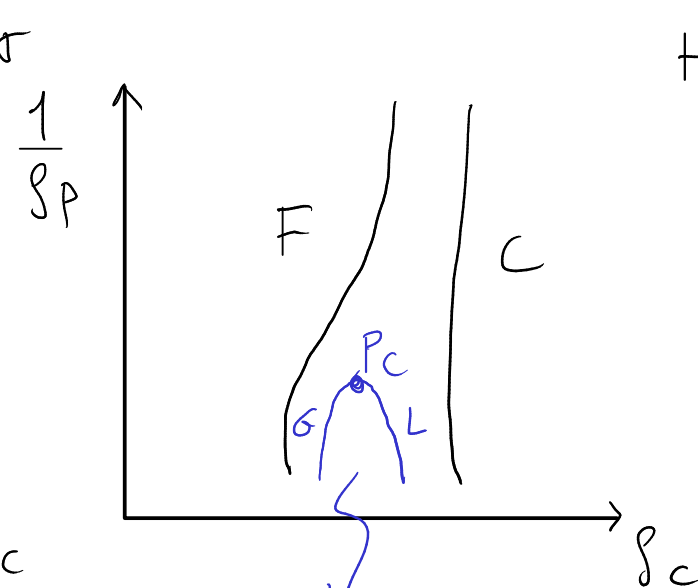
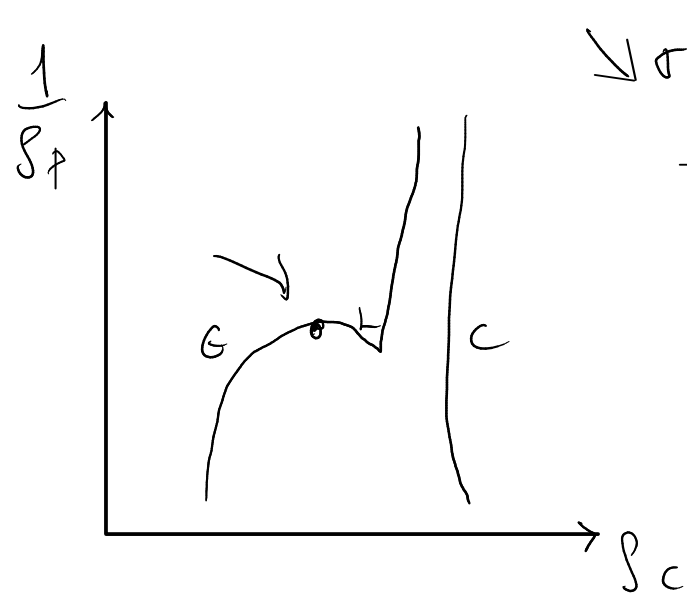
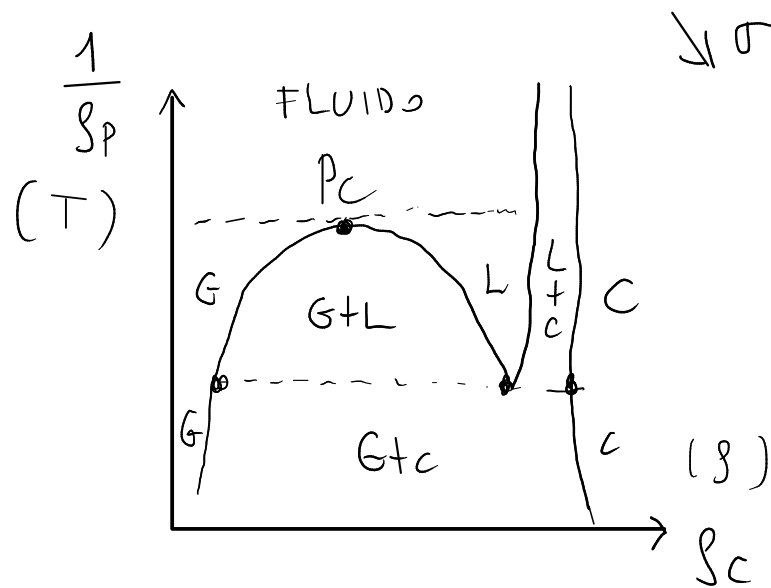
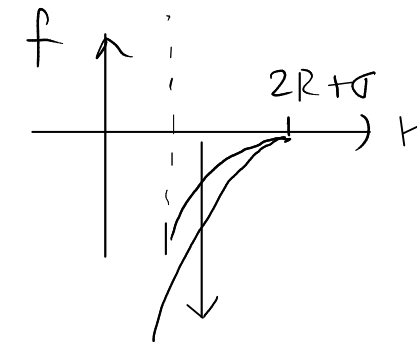


colloidi + polimeri ATERMICO

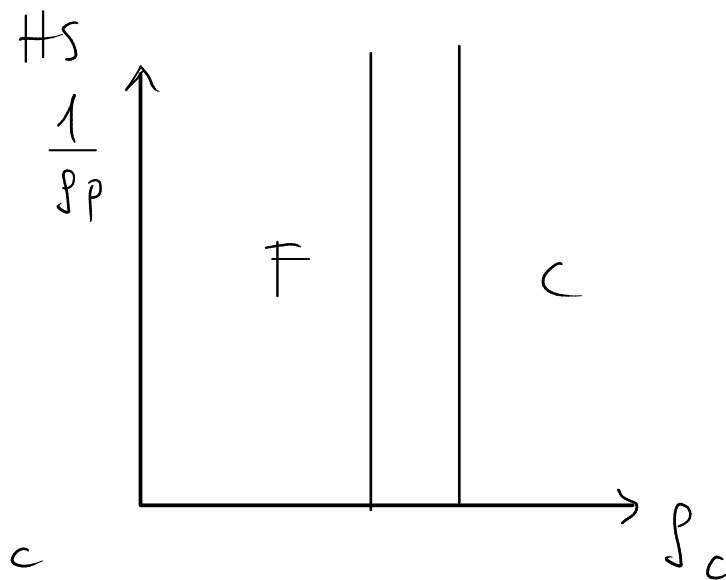
$$U_{\text{eff}}(r) = U_{\text{HS}}(r) + U_{\text{Ao}}(r) = \begin{cases} \infty & r \leq 2R \\ -k_{\text{BT}} \phi_p f(r) & r > 2R \end{cases}$$

$$\exp \left[-\frac{1}{k_{\text{BT}}} \sum_{ij} U_{\text{Ao}}(r_{ij}) \right]$$

$$\sim \exp \left[+\frac{1}{k_{\text{BT}}} \phi_p \sum_{ij} f(r_{ij}) \right]$$



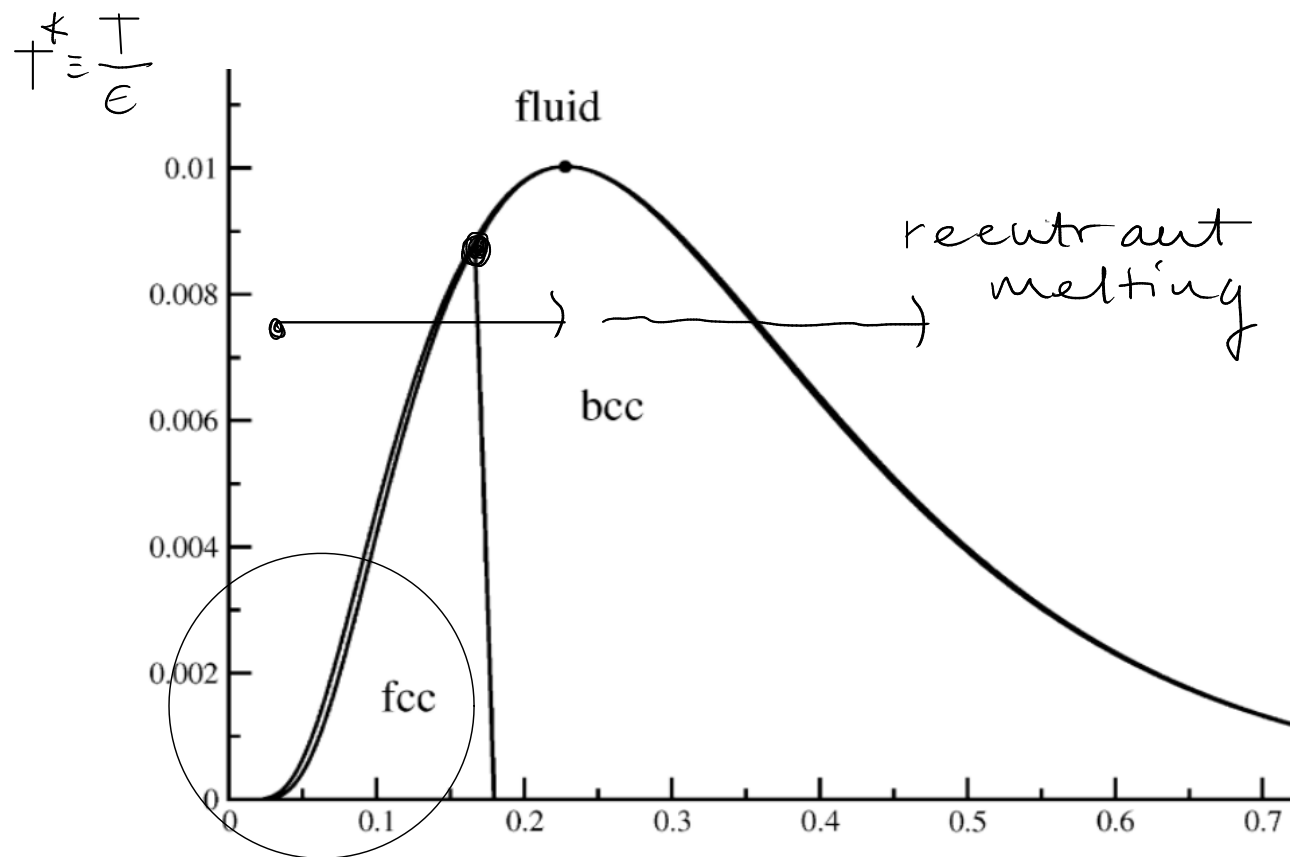
metastabile



3. colloidi ultrasoffici

Polimeri lineari, dendrimeri, microgels \rightarrow

ultrasoffice + bounded $U_{eff}(0) = cost$
ECM



Lang et al. 2000

$$\rho \sigma^3 \equiv \rho^*$$

$$\begin{cases} U(r) = \epsilon \exp[-(r/\sigma)^2] \\ \epsilon \sim k_B T \end{cases}$$

$$\epsilon = cost > 0$$

170 Stillinger

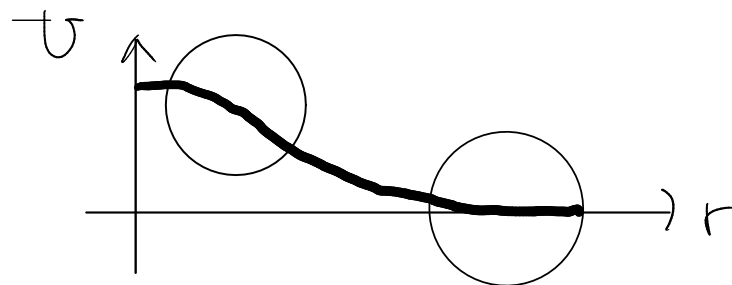


Diagramma fase GCM bassa β e T

$$B(r, T) = \exp \left[-\beta \underbrace{\epsilon \exp \left[-\left(\frac{r}{\sigma} \right)^2 \right]}_{U(r)} \right]$$

$$\left(r \rightarrow 0 \rightarrow B \approx \exp(-\beta \epsilon) \approx 0 \right.$$

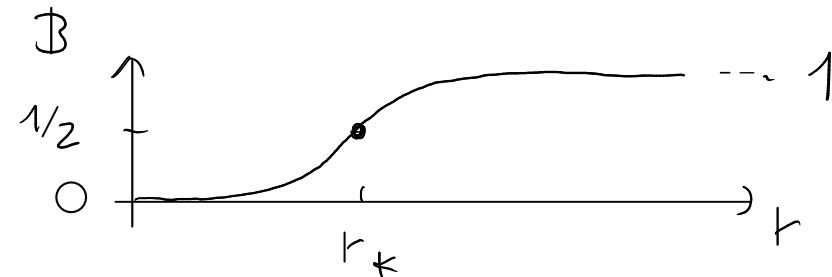
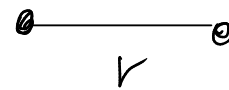
$$\left. r \rightarrow \infty \rightarrow B \approx 1 \right)$$

$$\frac{1}{2} = \exp \left[-\beta \epsilon \exp \left(-\left(\frac{r_k}{\sigma} \right)^2 \right) \right]$$

$$\ln 2 = \beta \epsilon \exp \left(-\left(\frac{r_k}{\sigma} \right)^2 \right)$$

$$\rightarrow \ln \left(\frac{\ln 2}{\beta \epsilon} \right) = -\left(\frac{r_k}{\sigma} \right)^2$$

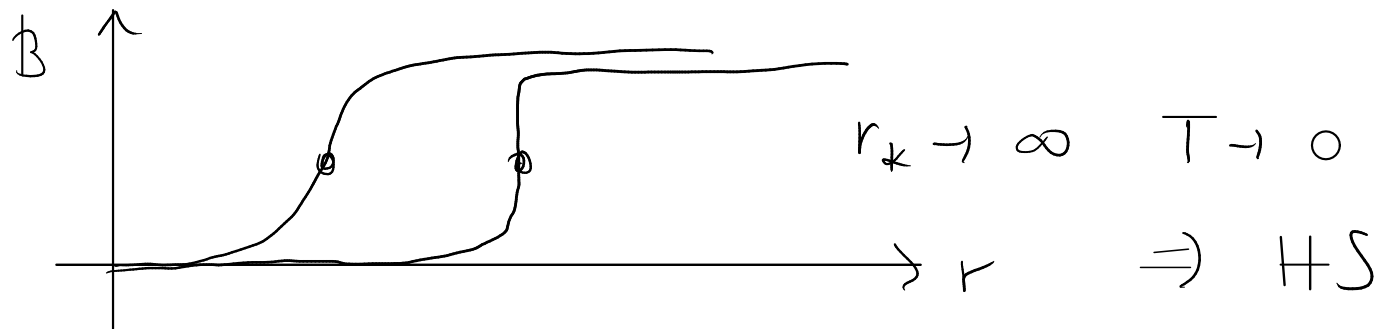
$$r_k = \sigma \sqrt{\ln \left(\frac{\beta \epsilon}{\ln 2} \right)}$$



$$B(r_k, T) = 1/2$$

$$\left. \frac{dB}{dr} \right|_{r_k} = \dots = \frac{r_k}{\sigma^2} \ln 2$$

(es.)



$$H_0: \phi_f = 0.49 \quad \phi_f = \frac{\pi}{6} \sigma^3 \rho_f = 0.49 \Rightarrow \sigma^3 \rho_f t_*^3 = 0.94$$

$$(\underline{es.}) \Rightarrow T_f \sim \exp\left(-\frac{0.94}{\rho_f^{2/3}}\right)$$

GEM : $U(r) = \epsilon \exp[-(r/\sigma)^n]$ $n \sim 3-4$

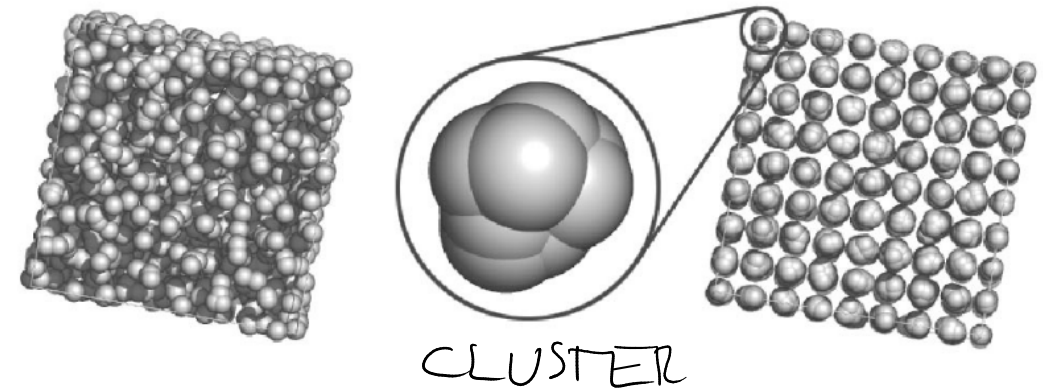
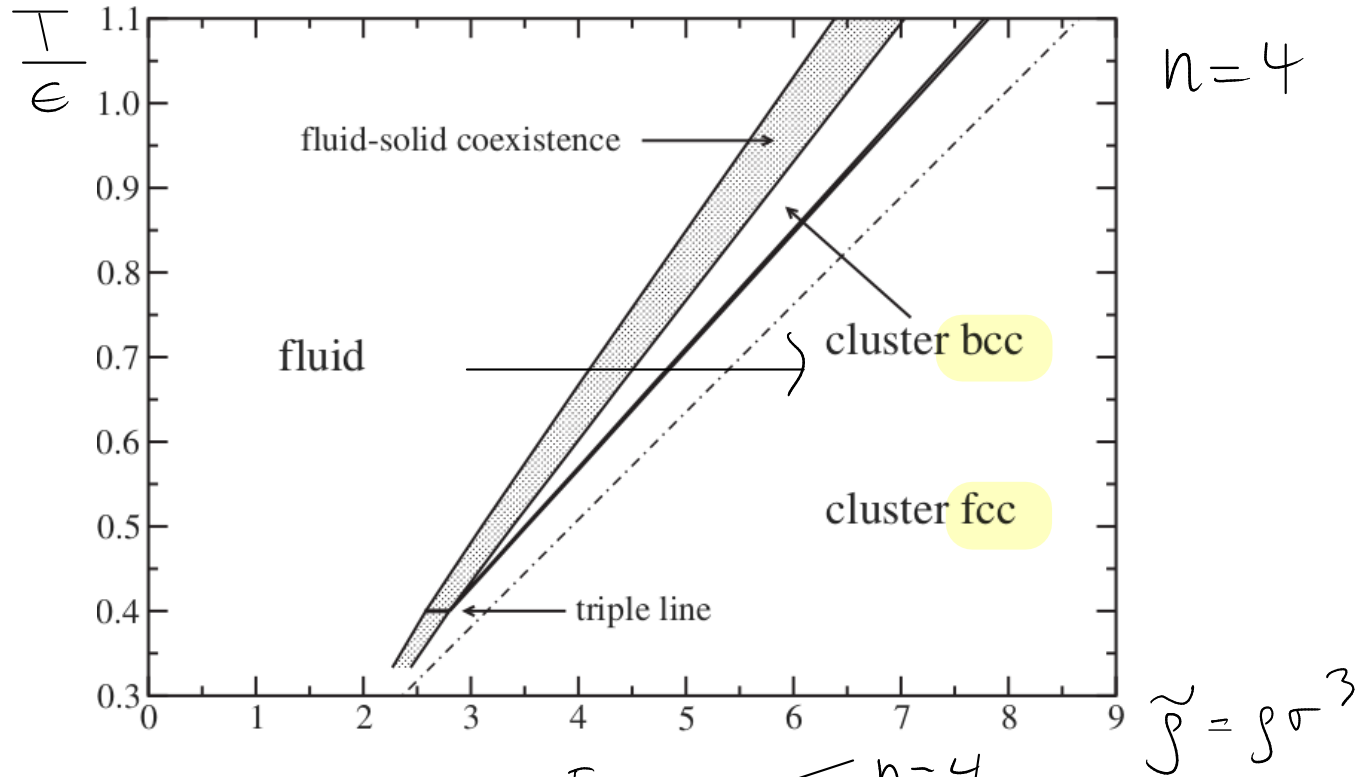
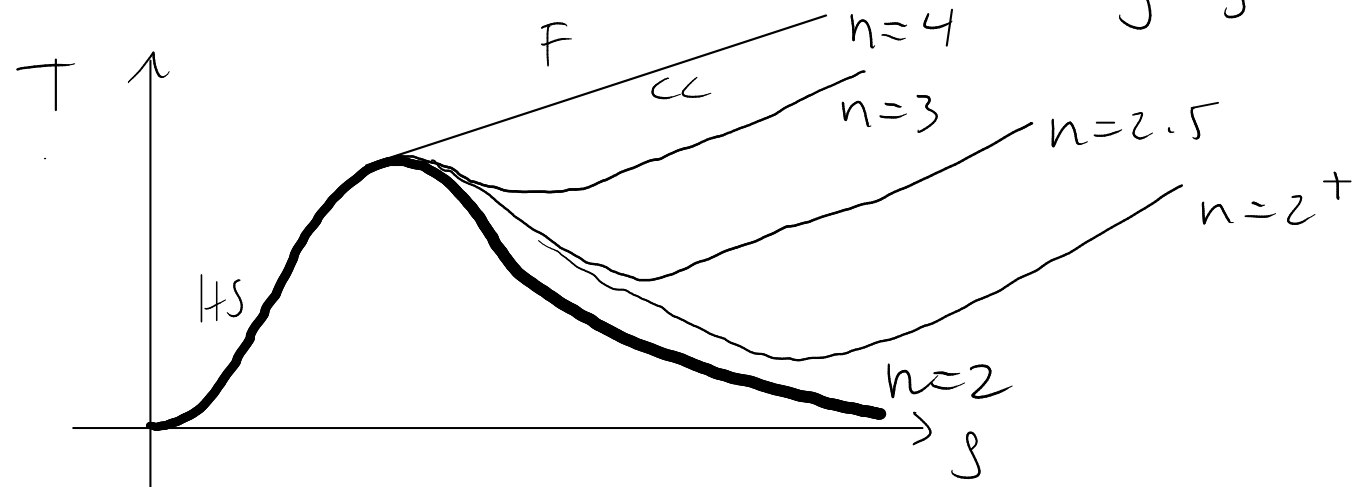


FIG. 2. Two simulation snapshots of a GEM-4 system for $T^* = 0.4$ and $\rho^* = 2.5$ and 7 (left and right). The middle panel shows a close-up of one cluster. Particle diameters are not drawn to scale but are chosen to optimize the visibility of the structures.

PRL **96**, 045701 (2006)



criterio di Likos

$$\exists k_k \text{ t.c. } \tilde{u}(k_k) < 0$$

\Rightarrow clusters

Self assembling cluster crystals from DNA based dendritic nanostructures

Emmanuel Stiakakis¹, Niklas Jung², Nataša Adžić³, Taras Balandin⁴, Emmanuel Kentzinger⁵, Ulrich Rücker⁵, Ralf Biehl⁶, Jan K. G. Dhont^{1,7}, Ulrich Jonas² & Christos N. Likos³

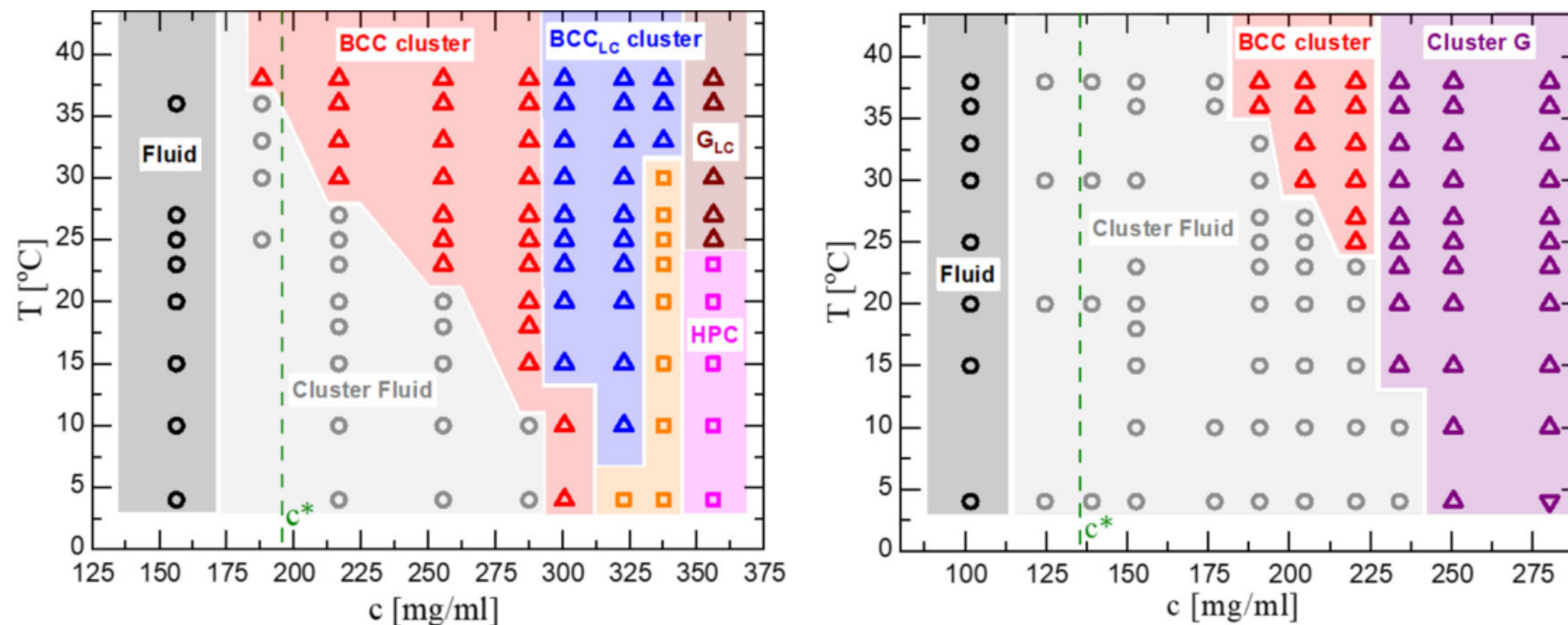


Fig. 6 Phase diagrams of G1-P-G1 and G2-P-G2. A concentration-temperature phase diagram of aqueous solutions of G1-P-G1 (a) and G2-P-G2 (b). The following phases are indicated: Fluid (black circles), cluster fluid (gray circles), BCC cluster crystal (red triangles), liquid crystalline BCC-like cluster crystal (BCC_{LC} cluster, blue triangles), liquid crystalline glass-like (G_{LC} , brown triangles), non-birefringent glass-like (Cluster G, purple triangles) and hexagonal packed cylinder (HPC, magenta squares). The corresponding background colors are added to assist in identifying the various phases. The structural assignment of the orange region in the G1-P-G1 phase diagram based solely on the SAXS data was not possible. The green-dashed lines indicate the DNA overlap concentration c^* of G1-P-G1 and G2-P-G2 (see Methods, “System parameters” section).